Spectroscopic ion beam imaging for investigations into magnetic field mapping of a plasma

D. R. Demers,[a] P. M. Schoch, and R. J. Radke
Rensselaer Polytechnic Institute, Troy, New York 12180

J. K. Anderson, D. Craig, and D. J. Den Hartog
University of Wisconsin, Madison, Wisconsin 53706

(Presented on 10 July 2002)

The trajectory of an ion beam as it passes through a magnetically confined plasma is determined by the ion mass, energy, and charge state, and the magnetic field structure. In undergraduate physics laboratories, students use a measure of beam deflection in a well-defined magnetic field to determine the charge-to-mass ratio of a particle. The complementary analysis is equally valid; the field may be determined given a known charge-to-mass ratio. Additional complexity is introduced in a spatially nonuniform, time-varying magnetic field, such as that of a plasma. The technique of field mapping via spectral imaging is being developed with a heavy ion beam probe on the Madison Symmetric Torus. Technical issues, such as choice of wavelengths, optics, viewing geometry, and imaging hardware, are being addressed. Calculations indicate that beam emission is brighter than background bremsstrahlung for several transitions of interest. However, a wavelength region containing lines from the beam ions, but free of atomic lines from the plasma, remains to be identified. © *2003 American Institute of Physics.* [DOI: 10.1063/1.1537439]

I. INTRODUCTION

Emission from beams has been used to measure various characteristics of magnetically confined plasmas, using diagnostics such as beam emission spectroscopy (BES) ($\tilde{n}$), charge exchange recombination spectroscopy (CHERS) (T_i), motional Stark effect (q, B). These emission measurements traditionally utilize a beam of neutral particles. Alternatively, the use of a charged-particle beam, which exhibits motion due to a magnetic field, would permit the characterization of the internal magnetic field of plasmas. This article aims to describe a concept and technique in the early stages of development. The concept is the inference of the magnetic field (B_p and B_t) of a magnetically confined plasma from the curvature of a singly charged particle beam moving through the field. The technique will utilize the spectroscopic observation of emission from the singly charged ions as they pass through the plasma. This technique will provide a direct, localized, time-resolved measurement, from plasma core to edge, that is not available from other diagnostics. This measurement may be of value to reversed field pinches (RFP) and to other alternative confinement devices in which heavy ion trajectories are highly three-dimensional (3D), and in which the magnetic fields are generated by currents in the plasma and are not known *a priori*. The method may also be of use for tracking changes in magnetic field with time in almost any magnetic confinement device.

II. PRINCIPLE OF LOCAL MAGNETIC FIELD MEASUREMENTS

Spectral imaging of a heavy ion beam to map the magnetic field profiles of a magnetically confined plasma, first proposed by Jobes and Peng,[1] has never before been attempted. This diagnostic technique will complement the well-established measurements of the heavy ion beam probe (HIBP).[2,3] As an HIBP's charged probing ions travel through a plasma, they are deflected by the confining magnetic field and may undergo electron impact excitation and electron impact ionization.[4] In practice, only a small fraction of the ions undergo electron impact ionization; these are the ions that are utilized in standard HIBP measurements. At the point of ionization, these doubly charged particles depart from the path of the singly charged ions (primaries). Most of the injected primary ions proceed along a well-defined path prescribed by the magnetic field, and are available to undergo electron impact excitation. Imaging the emission of excited primary ions will provide a map of trajectories and subsequently the deflection of the beam throughout the plasma. This deflection provides a measure of the magnitude and direction of the magnetic field from the Lorentz force equation, $m(dv/dt)=q(E+vxB)$. The magnitude of v and m are well known, the direction of v and dv/dt can be inferred from the image. E can be estimated from interior measurements of plasma potential (traditional HIBP measurement) and is generally small compared to the vxB term. The magnitude and direction of B can hence be computed.

The 3D nature of singly charged particle orbits within an RFP-type plasma is illustrated in Fig. 1. Beam trajectories vary with plasma current, beam energy, and beam injection angles. A trajectory may be moved within a plasma cross section by steering the beam or changing the beam energy. The example shown in Fig. 1(a) illustrates the poloidal projection of the orbits of primary sodium ions injected at three possible angles, and Fig. 1(b) is the corresponding orbit from a view above the midplane, demonstrating the toroidal de-

[a]Electronic mail: diane@ecse.rpi.edu

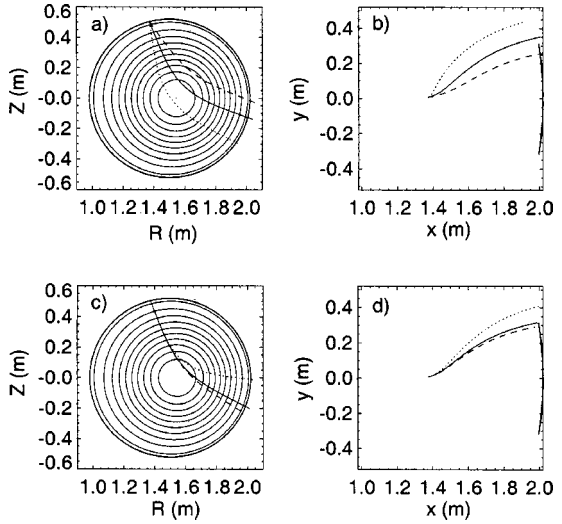

FIG. 1. The primary orbits of sodium ions injected at three possible angles. (a) The poloidal projection. (b) Viewed from above the midplane; the trajectories for one input angle but at beam energies of 40 (dotted), 70 (solid), and 90 (dashed) keV. (c) Poloidal cross section. (d) The orbits viewed from above.

flection. Alternatively, the primary ion energy can be changed to modify the trajectories. Shown in Figs. 1(c) and 1(d) are the trajectories for one input angle, but at beam energies of 40 (dotted), 70 (solid), and 90 (dashed) keV (poloidal and toroidal projections, respectively).

III. TECHNIQUE AND FEASIBILITY OF SPECTROSCOPIC MEASUREMENT

The success of this spectral imaging hinges on the ability to see the beam, and is largely dependent on two factors: (1) Will the beam emission intensity be strong enough for spectral imaging? and (2) Does the plasma have strong interfering spectral emission at the wavelengths of the probing ion lines?

A spectroscopic survey of the dominant emission lines from the Madison Symmetric Torus (MST)[5] RFP plasmas show no strong emission lines from singly ionized Na, K, Rb, Cs, or Tl (ions traditionally used by HIBPs). It is still necessary to choose emission lines that are not in the vicinity of dominant plasma radiation. In addition, the background radiation in the vicinity of these ion wavelengths must be sufficiently low to obtain a significant signal-to-noise ratio for the imaging application. Advantageous features of the probing ions include the large number of spectral lines, the strong line intensities, and the high number of lines within narrow ($\sim$10 nm) bandwidths. It is possible to simultaneously view groups of lines that will maximize the image intensity.

The intensity of the emission from the probing ion beam is highly dependent on the beam current density, which is related to the extracted beam current and the focus of the beam within the plasma. The present HIBP accelerating electrode configuration produces beams in the range of 20 to 100 μA. The beam diameter measured approximately 0.5 m below the end of the accelerating column is on the order of 0.5 cm full width at half maximum. The resulting beam density is on the order of 10^7-10^8 cm^{-3}. It is anticipated that a quadrupole lens will soon be added to the system, which will minimize the spread of the beam and maximize the density and localized emissivity along the trajectory line.

There are several other factors that influence the intensity of line emission from the beam ions. These include the energies/temperatures of the beam ions versus that of the plasma electrons, the variation in electron temperature and density along the ion orbit from the core to the edge, the attenuation of beam ions during transit, the fraction of ions that are ionized to higher charge states, and the fraction of ions that pass through the plasma without ionization or attenuation.

The dominant reaction channel for this spectral imaging application is expected to be electron impact excitation of the primary ions, while ionization, recombination, and others are relatively small. The following estimates indicate that the emission from the beam will be sufficiently bright for spectroscopic detection. As an example, we consider the emission from Na II (singly charged sodium ion), where collection of light is well suited at 295 ± 5 nm. In this wavelength band, a standard 10-nm-wide interference filter will collect light from 25 transitions.[6] The NIST atomic databases, tabulated relative intensity information, give an estimate that 24% of the total Na II line radiated power is through this series of transitions. The rate of photons produced per unit volume is $r=n_e n_i\langle\sigma v\rangle$, where σ is the total cross section for electron impact excitation of the beam ions, v is the thermal speed of the plasma electrons (much greater than the speed of the beam ions), and n_e and n_i are the densities of the plasma electrons and beam ions, respectively. The background electron density in MST is on the order of 10^{13} cm^{-3}, and the beam ion density is approximately 10^8 cm^{-3}. The total cross section for electron impact excitation is estimated from simple considerations; a lower bound is obtained using published values of the electron impact excitation cross section for the analogous set of transitions in neutral neon, which has the same electronic structure as Na II.[7] A conservative estimate is $\sigma\sim60\times10^{-20}$ cm^2 at $T_e=200$ eV (or $v_{\text{the}}\sim8\times10^8$ cm/s). The actual cross section for Na II is presumably higher because the positive ionic charge increases the likelihood of interaction with background electrons. All considered, the emissivity is expected to exceed 75 nW cm^{-3}. This emissivity is significantly stronger than the background bremsstrahlung and neutral deuterium (D, D_2) emission, which dominate the MST continuum.[8] A similar analysis of the cesium ion, which has a significantly larger cross section[9] than the sodium ion, results in a factor of 2 increase in the expected emissivity. Furthermore, there are several intense Cs II lines near 523 nm, a region free of impurity lines in MST.

Existing filtering techniques can be utilized to preclude contamination from the extremely bright deuterium lines (particularly D_α), which are several orders of magnitude brighter. Background emission increases by about an order of magnitude in the MST at the sawtooth crash. Imaging between these discrete events will further improve the signal-to-noise ratio. Initial tests will use a spectrometer to verify and identify the lines of strongest intensity. The imaging will

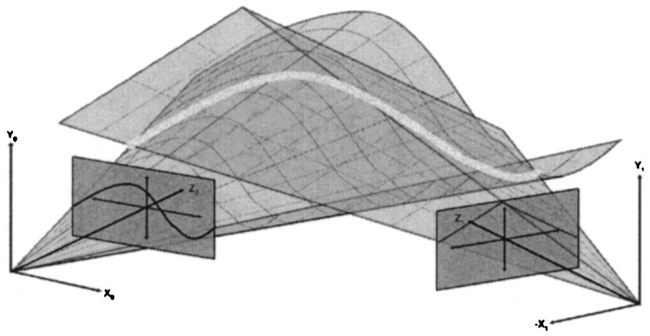

FIG. 2. The three-dimensional trajectory of the ion beam can be reconstructed from the beam's projection onto two image planes.

then utilize bandpass filters sensitive to the identified wavelengths.

IV. IMAGING THE BEAM TRAJECTORY

The final system will image the primary beam with a CCD camera from two vantage points: one will acquire a poloidal projection of the beam trajectory, the other a toroidal projection. The spatial resolution of the camera and the resulting beam image are important for accurate field mapping. Although a camera has not yet been acquired, a survey of those suitable for the application suggests that the resolution of the image will be better than 0.25 cm^2. A camera that can acquire multiple images throughout a shot will be chosen. Images will be acquired continuously throughout the plasma discharge, producing a time history of the plasma trajectory and thus of the magnetic field structure.

During the multiviewpoint phase of development, it will be a challenge to spatially align the images. Accurate camera calibration is required to compute precise 3D trajectories, and the placement of fiducial marks within the MST chamber may be beneficial for the initial calibration. MST wall elements may also serve as landmarks if they exist in fortuitous locations. If necessary, the images can be projectively warped to bring the fiducials in line with a prior model of the MST.[10] With the positions of the cameras accurately determined, the 3D trajectory of the ion beam can be reconstructed from the projection of the beam onto two image planes.[11] Figure 2 illustrates the process, assuming ideal perspective-projection cameras. The projection of the ion trace onto the image plane of the left-hand camera (here, a wavy line) induces a two-dimensional (2D) surface in 3D space on which the ion beam is constrained to lie. The projection of the beam onto the second camera (here, a rooftop shape) induces another such surface. In the general case, these two surfaces will intersect in a one-dimensional path through 3D space. Only one beam trajectory is consistent with both projections, represented here by a thick white line.

The consistency of the local magnetic field measurement may be evaluated by combining the techniques described in Sec. II, Fig. 1. The beam energy and injection angle can be varied over the course of many shots. The beam energy can only be changed on a shot-to-shot basis. Thus, during one shot, the beam energy will be fixed and the injection angle will be scanned. The process of incrementing the beam energy and scanning the injection angle will be repeated over many shots. The curvature of the beam during the various shots will differ due to the different ion velocity vectors, but the sampling will cross the same regions. The consistency check inherent in this technique is that the local measurements should be the same for the different ion energies.

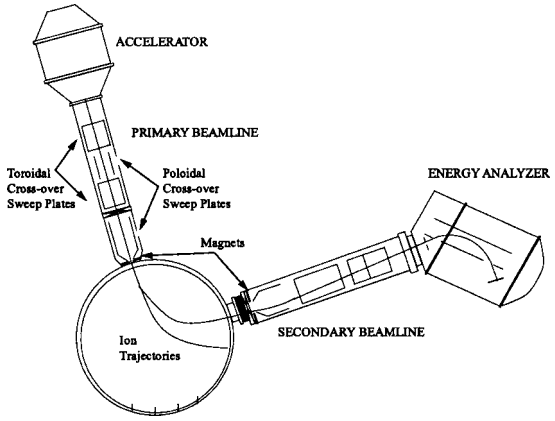

FIG. 3. A cross-sectional view of the HIBP installed on MST.

Additionally, the plots in Fig. 1 serve to illustrate that constraining the magnetic equilibrium via the position of the primary orbit on the opposing wall would be impractical due to the vast area of the wall that is impacted by primary ions. While this technical challenge could be overcome, the information provided is much more limited than that provided by the trajectory image. This wall imaging technique may be used in parallel with beam imaging, but at strategically selected wall locations.

V. EXPERIMENTAL SETUP AND PLANS

An HIBP[12,13] is in operation on the MST. MST has a major radius of 1.5 m, a minor radius of 0.52 m, and an inner machine surface of aluminum with some graphite and ceramic protection tiles. Typical MST plasmas are in the range of $I_p = 200-500$ kA, $n_e = 0.5-1.5\times10^{13}$ cm^{-3}, and $T_e < 1$ keV. The background gas is deuterium.

The HIBP on the MST is designed to operate with beam energies of up to 200 keV, but most commonly operates with energies less than 90 keV. A singly charged ion beam is injected into a discharge, which typically lasts on the order of 60 ms. Electrostatic steering plates within the primary (injection) beam line are capable of injecting a beam with deflections of $\pm20°$ in the poloidal direction and $\pm5°$ in the toroidal direction.[14] It is with these sweep plates that the beam is scanned across a portion of the plasma cross section during a shot. Figure 3 is a cross-sectional image of the HIBP installed on the MST.

This machine and diagnostic pairing are well-suited for the development of this beam imaging technique for the following reasons. (1) The comparable magnitudes of the RFP's toroidal and poloidal magnetic fields cause the probing ion trajectories to undergo both significant poloidal and toroidal deflection. The 3D nature of the orbit presents an interesting opportunity for multiviewpoint imaging and 3D field mapping. (2) A variety of poloidally and toroidally displaced ports are available for beam imaging. (3) A large fraction of

the plasma cross section, from the core to the edge, is accessible to probing ions, thus providing a variety of trajectories to be mapped. (4) The magnetic field profiles of the RFP are not well known, but are of considerable interest to current profile control studies. (5) A significant effort in equilibrium profile reconstruction is ongoing at MST. The field modeling and imaged-field mapping may be benchmarked against each other, and the field maps may be used as constraints in the equilibrium reconstruction code.

An immediate goal is to determine the brightest spectral lines from beam ions that are not masked by conventional plasma emission. This will be done via a broad spectral survey of various beam ions; beams will be injected into the plasma and the spectra recorded with a spectrometer. Since the ultimate goal is to image the beam, it is not necessary to choose one spectral line. The ideal situation would be to choose an isolated grouping of lines; this would permit the use of a narrowband filter to maximize the brightness of the imaged trajectory.

The spectral survey will encompass a range of wavelengths, 250–750 nm, necessitating the use of fused silica windows. Two such windows presently exist on the MST. The first, a 4.5 in. port with optics, window, and protective rotatable shutter (to prevent window coating) exists at a location displaced 85° toroidally from the beam injection port. A ray tracing code has been used to determine the appropriate fiber optic placements relative to the port optics to detect a variety of beam emission wavelengths. In addition, a second window was recently installed on a 1.5 in. port that is displaced 10° toroidally from the beam injection port. Plans also exist to install one additional window and optics on a 2 in. port on the outboard side of the machine. A CCD camera mounted on the output slit of a 0.5 m spectrometer with a 150-grooves-per-mm grating will be used to survey approximately 105 nm of the spectrum onto its 750 pixels. Finer spectral resolution of the line groupings of interest will be obtained with a second grating of 1800 grooves per mm (7.5 nm per 750 pixels). The spectrometer is triggered by the MST control system; trigger and dwell times are adjustable.

Subsequent to the spectral survey will be the selection of ports from which the beam will be imaged, and the design of optics suitable for the imaging. A preliminary study suggests that the design will place the viewing optics into the 5-cm-thick aluminum port (wall) of the machine. This type of optics placement will maximize the field of view. A shutter system that covers the viewing optics when not in use will also be necessary to prevent coating of the lenses during routine machine operation and conditioning. The survey will also guide the purchase of suitable CCD camera and filters.

VI. FUTURE WORK

It is anticipated that subsequent development will progress in stages. First, a single camera will be installed and integrated into the general machine trigger and data acquisition system. Next, spectroscopic images will be acquired from a single port, allowing for optics and filter design to be adjusted if necessary before implementation on a second port. The additional imaging issues, such as the evaluation of MST wall landmarks and the insertion of fiducials on the machine inner surface, will be addressed as well. Extraction of 2D field information from the single camera images and the interface of the 2D spectroscopic field data with the MSTFit equilibrium modeling code will begin.

A cursory outline of longer-term plans includes the purchase and installation of a second CCD camera, the acquisition of multiview spectroscopic camera images, and the development of code to utilize the 2D spectroscopic data in the generation of 3D images and field maps.

It is certain that additional detailed consideration must also be given to investigating the effects of fluctuations and magnetohydrodynamic measurements, imaging during sawtooth cycles (may require higher frame rates), testing for electric field effects on the trajectories, and surveying alternative spectroscopic beam imaging enhancements such as scintillators, phosphor screens, edge arrays, and framing cameras.

ACKNOWLEDGMENT

This work is supported by the U.S. DOE.

[1] F. C. Jobes and M. Peng, Bull. Am. Phys. Soc. **42**, 1990 (1997).
[2] V. J. Simcic, T. P. Crowley, P. M. Schoch, A. Y. Aydemir, X. Z. Yang, K. A. Connor, R. L. Hickok, A. J. Wootton, and S. C. McCool, Phys. Fluids B **5**, 1576 (1993).
[3] T. P. Crowley, Rev. Sci. Instrum. **59**, 1638 (1988).
[4] J. G. Schwelberger and K. A. Connor, IEEE Trans. Plasma Sci. **22**, 418 (1994).
[5] J. N. Tabora, D. Craig, and D. J. Den Hartog, MST internal report PLP1234, Plasma Studies, University of Wisconsin-Madison, August 2000.
[6] Online ''lines'' database at [http://physics.nist.gov/cgi-bin/AtData/main_asd].
[7] J. E. Chilton, M. D. Stewart, and C. C. Lin, Phys. Rev. A **61**, 052708 (2000).
[8] J. K. Anderson, Ph.D. thesis, University of Wisconsin, Madison, 2001.
[9] J. T. Fons and C. C. Lin, Phys. Rev. A **58**, 4603 (1998).
[10] R. Radke, P. Ramadge, T. Echigo, and S. Iisaku, Proceedings of the IEEE ICIP 2000, Vancouver, Canada, Sept. 2000.
[11] R. Hartley and A. Zisserman, *Multiple View Geometry in Computer Vision* (Cambridge University Press, Cambridge, UK 2000).
[12] D. R. Demers, J. Lei, U. Shah, P. M. Schoch, K. A. Connor, T. P. Crowley, J. G. Schatz, J. K. Anderson, and J. S. Sarff, Czech. J. Phys. **51**, 1065 (2001).
[13] J. Lei, U. Shah, D. R. Demers, K. A. Connor, and P. M. Schoch, Rev. Sci. Instrum. **72**, 564 (2001).
[14] J. Lei, T. P. Crowley, U. Shah, P. M. Schoch, K. A. Connor, and J. Schatz, Rev. Sci. Instrum. **70**, 967 (1999).